

FLUID FLOW AND HEAT TRANSFER IN A COLLAPSIBLE TUBE

S. A. ODEJIDE¹, Y. A. S. AREGBESOLA¹, O. D. MAKINDE²

¹ Obafemi Awolowo University, Department of Mathematics, Faculty of Science, Ile-Ife, Nigeria

² Applied Mathematics Department, Private Bag X1106, Sovenga 0727, South Africa

Received February 13, 2007

In this paper, we examined an incompressible viscous fluid flow and heat transfer in a collapsible tube. The non linear equation arising from the model were solved using perturbation series. An increasing or decreasing in the Prandtl number leads to increasing or decreasing in the rate of heat transfer across the wall.

AMS Subject Classification: 78M20, 74G15, 76E25.

Key words: incompressible viscous fluid, collapsible tube, perturbation series, heat transfer.

1. INTRODUCTION

Fluid flow through collapsible tubes is a complex problem due to the interaction between the tube-wall and the flowing fluid, Heil (1997). Collapsible tubes are easily deformed by negative transmural pressure owing to marked reduction of rigidity. Hence, they show a considerable nonlinearity and reveal various complicated phenomena. They are usually used to simulate biological flows such as blood flow in arteries or veins, flow of urine in urethras and air flow in the bronchial airways. They can also be used to study and prediction of many diseases, as the lung disease (asthma and emphysema), or the cardiovascular diseases (heart stroke), Makinde (2005).

In this work, laminar flow of an incompressible viscous fluid through a collapsible tube of circular cross section is considered. Our objectives are to study the effect of temperature along the tube as the fluid Prandtl number and Reynolds number increases. Also to examine the rate of heat transfer across the wall.

In Section 2, we establish the mathematical formulation of the problem. Graphical interpretation and discussion of the pertinent results were presented in Section 3.

2. MATHEMATICAL FORMULATION

Let consider the transient flow of a viscous incompressible fluid in a collapsible tube. We take a cylindrical polar coordinate system (r, θ, z) where oz

lies along the center of the tube, r is the distance measured radially and θ is the azimuthal angle. Let u and v be the velocity components in the directions of z and r increasing respectively.

Assume $r = a_0\sqrt{(1-\alpha t)}$, where α is a constant of dimension $[T^{-1}]$ which characterizes unsteadiness in the flow field, a_0 is the characteristic radius of the tube at time $t = 0$ as shown in the figure below.

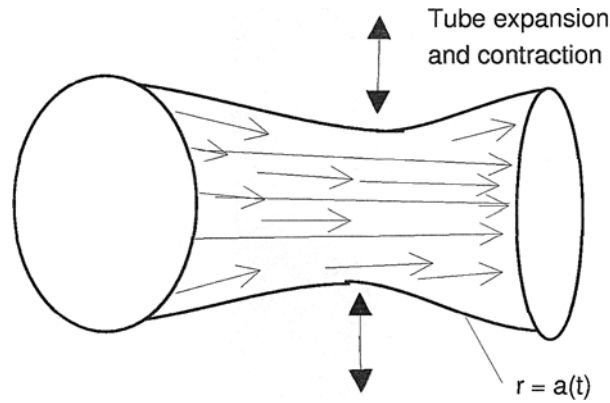


Fig. 1 – Geometry of the problem.

For axisymmetric unsteady viscous incompressible flow, the governing equations are as follows:

Continuity equation

$$\frac{\partial(rv)}{\partial r} + r \frac{\partial u}{\partial z} = 0, \quad (1)$$

Navier-Stokes equations

$$\frac{\partial u}{\partial t} + u \frac{\partial u}{\partial z} + v \frac{\partial u}{\partial r} = \frac{-1}{\rho} \frac{\partial p}{\partial z} + \nu \nabla^2 u, \quad (2)$$

$$\frac{\partial v}{\partial t} + u \frac{\partial v}{\partial z} + v \frac{\partial v}{\partial r} = \frac{-1}{\rho} \frac{\partial p}{\partial r} + \nu (\nabla^2 u - \frac{v}{r^2}), \quad (3)$$

Energy equation

$$\rho c_p \left\{ \frac{\partial T}{\partial t} + u \frac{\partial T}{\partial z} + v \frac{\partial T}{\partial r} \right\} = K \nabla^2 T, \quad (4)$$

where $\nabla^2 = \frac{\partial^2}{\partial r^2} + \frac{1}{r} \frac{\partial}{\partial r} + \frac{\partial^2}{\partial z^2}$, p is the pressure, ρ the density, ν the kinematic viscosity of the fluid, T is the temperature, K the coefficient of thermal

conductivity, μ the coefficient of viscosity and c_p is the specific heat capacity at constant pressure.

The appropriate boundary conditions are:

Regularity of solution along z - axis *i.e.*

$$\frac{\partial u}{\partial r} = 0, \quad v = 0, \quad \frac{\partial T}{\partial r} = 0, \quad \text{on } r = 0 \quad (5)$$

The axial and normal velocities at the wall are prescribed as:

$$u = 0, \quad v = \frac{\partial a}{\partial t}, \quad T = \frac{T_0 z}{a_0 \sqrt{1 - \alpha t}}, \quad \text{on } r = a(t). \quad (6)$$

Introducing the stream function ψ and vorticity ω as follows:

$$u = \frac{1}{r} \frac{\partial \psi}{\partial r} \quad \text{and} \quad v = \frac{-1}{r} \frac{\partial \psi}{\partial z} \quad (7)$$

$$\omega = \frac{\partial v}{\partial z} - \frac{\partial u}{\partial r} = \frac{-1}{r} \frac{\partial^2 \psi}{\partial z^2} - \frac{1}{r} \frac{\partial^2 \psi}{\partial r^2} + \frac{1}{r^2} \frac{\partial \psi}{\partial r} \quad (8)$$

Eliminating pressure p from (2) and (3) by using (7) and (8), we obtain

$$\frac{\partial \omega}{\partial t} + \frac{1}{r} \frac{\partial(\psi, \omega)}{\partial(r, z)} + \frac{\omega}{r^2} \frac{\partial \psi}{\partial z} = \nu \left[\nabla^2 \omega - \frac{\omega}{r^2} \right], \quad \omega = -\nabla^2 \psi \quad (9)$$

Also, using (7) in (4), we have

$$\frac{\partial T}{\partial t} + \frac{1}{r} \frac{\partial(\psi, T)}{\partial(r, z)} = \frac{K}{\rho c_p} \nabla^2 T. \quad (10)$$

The boundary conditions become

$$\frac{\partial \psi}{\partial r} = 0, \quad \frac{\partial \psi}{\partial z} = -a \frac{da}{dt}, \quad T = \frac{T_0 z}{a_0 \sqrt{1 - \alpha t}}, \quad r = a(t) \quad (11)$$

$$\frac{\partial}{\partial r} \left(\frac{1}{r} \frac{\partial \psi}{\partial r} \right) = 0, \quad \frac{\partial \psi}{\partial z} = 0, \quad \frac{\partial T}{\partial r} = 0, \quad r = 0. \quad (12)$$

Introducing the following transformations:

$$\eta = \frac{r}{a_0 \sqrt{1 - \alpha t}}, \quad \psi = \frac{a_0^2 \alpha z F(\eta)}{2}, \quad \omega = \frac{-\alpha z G(\eta)}{2 a_0 (\sqrt{1 - \alpha t})^3}, \quad T = \frac{T_0 z \theta(\eta)}{a_0 \sqrt{1 - \alpha t}}. \quad (13)$$

Substituting (13) into equations (9)–(12), we have

$$\frac{d}{d\eta} \left[\frac{1}{\eta} \frac{d(\eta G)}{d\eta} \right] = R \left[\frac{G}{\eta} \frac{dF}{d\eta} - F \frac{d}{d\eta} \left(\frac{G}{\eta} \right) + \eta \frac{dG}{d\eta} + 3G \right], \quad G = \frac{d}{d\eta} \left[\frac{1}{\eta} \frac{dF}{d\eta} \right] \quad (14)$$

$$\frac{d}{d\eta} \left(\eta \frac{d\theta}{d\eta} \right) = PR \left[\theta \frac{dF}{d\eta} - F \frac{d\theta}{d\eta} + \eta^2 \frac{d\theta}{d\eta} + \eta\theta \right], \quad (15)$$

$$\frac{d}{d\eta} \left[\frac{1}{\eta} \frac{d(\eta G)}{d\eta} \right] = 0, \quad F = 0, \quad \frac{d\theta}{d\eta} = 0 \quad \text{on } \eta = 0, \quad (16)$$

$$\frac{dF}{d\eta} = 0, \quad F = 1, \quad \theta = 1 \quad \text{on } \eta = 1, \quad (17)$$

where $R = \frac{a_0^2 \alpha}{2\nu}$ is the Reynolds number and $PR = \frac{\rho c_p a_0^2 \alpha}{2K}$ is the product of Prandtl number and Reynolds number (*i.e.* Peclet number).

We now solve equations (14)–(17) by assuming a power series expansion, for small Reynolds number, of the form

$$F = \sum_{i=0}^{\infty} F_i R^i, \quad G = \sum_{i=0}^{\infty} G_i R^i \quad \text{and} \quad \theta = \sum_{i=0}^{\infty} \theta_i R^i. \quad (18)$$

Substituting equation (18) into equations (14)–(17) and collecting the coefficients of like powers of R , we have the following: zeroth order and higher order equations as in appendix A1.

We have written a MAPLE program that calculates successively the coefficients of the solution series. In outline, it consists of the following segments:

1. Declaration of arrays for the solution series coefficients *e.g.* $F = \text{array}(0..10)$, $G = \text{array}(0..10)$, $\theta = \text{array}(0..10)$.
2. Input the leading order term and their derivatives *i.e.* F_0, G_0, θ_0 .
3. Using MAPLE loop procedure to solve equations (23)–(26) (in Appendix A1) for the higher order terms *i.e.* F_n, G_n and θ_n , $n = 1, 2, 3, \dots$

Details of the MAPLE program can be found in Appendix A2.

3. GRAPHICAL RESULTS AND CONCLUSION

In our numerical calculation, we have used different Prandtl numbers such as air ($P = 0.71$), water ($P = 7.1$) etc. Fig. 2 and Fig. 3 show that the fluid temperature increases with an increase in fluid Prandtl number with maximum value at the center. In Fig. 4, we fixed the Prandtl number and varying the Reynolds number. An increase in Reynolds number leads to an increase in the fluid temperature with maximum magnitude at the pipe center and minimum at the wall. Fig. 5 and Fig. 6 show the rate of heat transfer across the wall. For $R < 0$ (wall expansion), as the Prandtl number increases the rate of heat transfer

increases. Also, for $R > 0$ (wall contraction), the rate of heat transfer decreases with increases in the Prandtl number. Fig. 7 shows the fluid velocity profile which is parabolic in nature and increases as Reynolds number increases.

From our analysis, it is important to note that wall expansion is represented by negative values of flow Reynolds number ($R < 0$) while wall contraction is

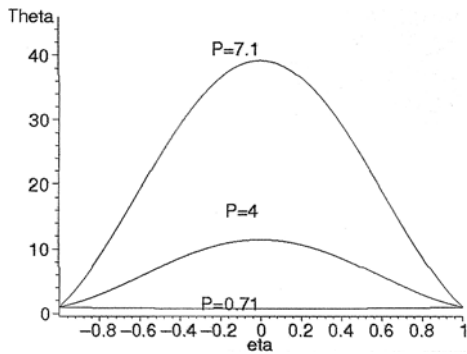


Fig. 2 – θ vs. η for $R = 1$.

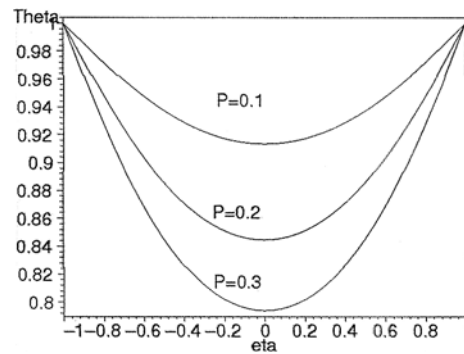


Fig. 3 – θ vs. η for $R = 1$.

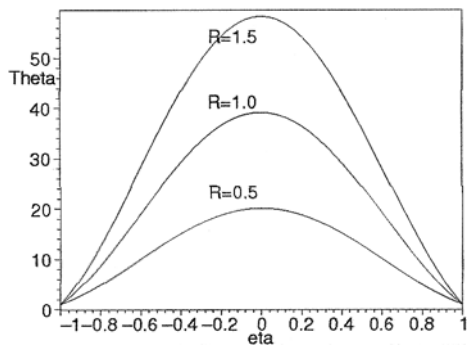


Fig. 4 – θ vs. η for $P = 7.1$.

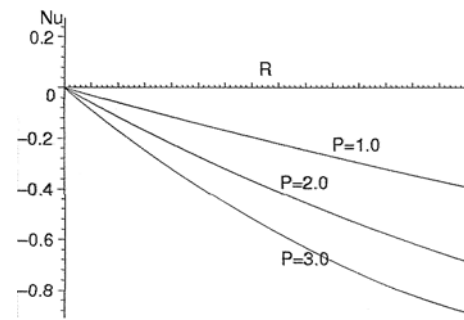


Fig. 5 – Nu vs R .

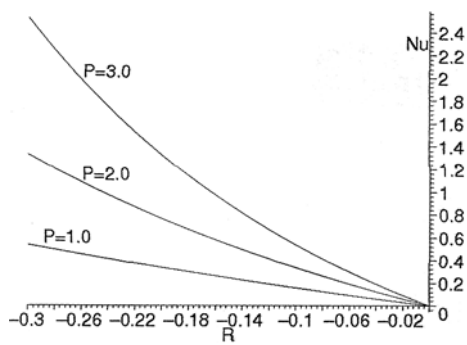


Fig. 6 – Nu vs R .

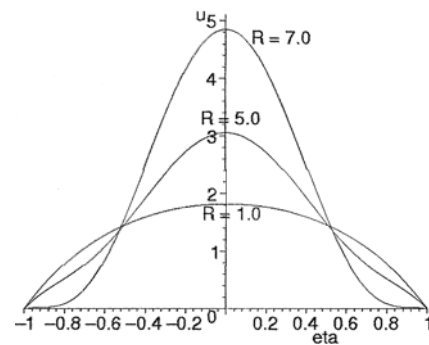


Fig. 7 – u vs η .

represented by positive values of flow Reynolds number ($R > 0$). It is interesting to note that the fluid temperature increases transversely with maximum value along the channel centerline for fluid with Prandtl number greater than or equal to one whereas the opposite is observed *i.e.* a transverse decrease in temperature, for fluid with Prandtl number less than one (Figs. 2–3). Furthermore, it is observed that the fluid temperature increases with increasing positive values of flow Reynolds number ($R > 0$) as illustrated in Fig. (4). In Figs. (5-6), the wall heat flux is illustrated for both positive and negative values of flow Reynolds number. It is noteworthy that for $R > 0$, the rate of heat transfer across the wall decreases with increasing values of Prandtl number (P) whereas for $R < 0$, the wall heat flux increases with increasing values of Prandtl number. Finally, we observed that the fluid velocity increases with increasing positive values of flow Reynolds number.

APPENDIX

A1: Zeroth Order

$$\frac{d}{d\eta} \left(\frac{1}{\eta} \frac{d(\eta G_0)}{d\eta} \right) = 0, \quad G_0 = \frac{d}{d\eta} \left(\frac{1}{\eta} \frac{d(F_0)}{d\eta} \right) = 0. \quad (19)$$

$$\frac{d}{d\eta} \left(\eta \frac{d(\theta_0)}{d\eta} \right) = 0, \quad (20)$$

$$\frac{d}{d\eta} \left(\frac{1}{\eta} \frac{d(F_0)}{d\eta} \right) = 0, \quad F_0 = 0, \quad \frac{d\theta_0}{d\eta} = 0, \quad \text{on } \eta = 0 \quad (21)$$

$$\frac{dF_0}{d\eta} = 0, \quad F_0 = 1, \quad \theta_0 = 1 \quad \text{on } \eta = 1 \quad (22)$$

Higher Order ($n \geq 1$):

$$\frac{d}{d\eta} \left(\frac{1}{\eta} \frac{d(\eta G_n)}{d\eta} \right) = \sum_{i=0}^{n-1} \left(\frac{G_i}{\eta} \frac{dF_{n-i-1}}{d\eta} - F_i \frac{d}{d\eta} \left(\frac{G_{n-i-1}}{\eta} \right) + \eta \frac{dG_{n-1}}{d\eta} + 3G_{n-1} \right), \quad (23)$$

$$G_n = \frac{d}{d\eta} \left(\frac{1}{\eta} \frac{d(F_n)}{d\eta} \right),$$

$$\frac{d}{d\eta} \left(\eta \frac{d\theta_n}{d\eta} \right) = P \left[\sum_{i=0}^{n-1} \left(\theta_i \frac{dF_{n-i-1}}{d\eta} - F_i \frac{d\theta_{n-i-1}}{d\eta} \right) + \eta^2 \frac{d\theta_{n-1}}{d\eta} + \eta \theta_{n-1} \right], \quad (24)$$

$$\frac{d}{d\eta} \left(\frac{1}{\eta} \frac{d(F_n)}{d\eta} \right) = 0, \quad F_n = 0, \quad \frac{d\theta_n}{d\eta} = 0, \quad \text{on } \eta = 0 \quad (25)$$

$$\frac{dF_n}{d\eta} = 0, \quad F_n = 0, \quad \theta_n = 0 \quad \text{on} \quad \eta = 1. \quad (26)$$

A2: The MAPLE procedure to solve the equations (23)–(26)

```
# Declare the arrays to store the computed results
F := array(0..10), G := array(0..10), theta := array(0..10), Feta := array(0..10),
Geta := array(0..10), theteta := array(0..10);

# Input the zero order solution F[0], G[0] and theta[0].
F[0] := (2 * eta^2 - eta^4) : G[0] := -8 * eta : theta[0] := 1 :
Feta[0] := diff(F[0], eta) : Geta[0] := diff(G[0], eta) : theteta[0] := diff(theta[0], eta) :

# Compute the higher order terms, n > 0,
for n from 1 by 1 to 10 do
A1 := normal(1/eta * sum(G[i] * Feta[n - i - 1] + F[i] * (G[n - i - 1]/eta -
Geta[n - i - 1]), i = 0..n - 1)) :
A2 := normal(eta * Geta[n - 1] + 3 * G[n - 1]) :
A := R * (A1 + A2) : A1 := 0 : A2 := 0 : g11 := normal(eta * (int(A, eta) + K)) :
A := 0 : g1 := normal(int(g11, eta)/eta) :
g11 := 0 : f11 := normal(eta * (int(g1, eta) + M)) :
f1 := normal(int(f11, eta)) : B := normal(P * R * sum((theta[i] * Feta[n - i - 1]
- F[i] * theteta[n - i - 1]) + eta * theta[n - 1] + eta^2 * theta[n - 1]), i = 0..n - 1)) : t11 :=
normal((int(B, eta)/eta)) : B := 0 : t1 := normal(int(t11, eta) + L) : eta := 1 : K :=
normal(solve(f11 = 0, K)) : M := normal(solve(f1 = 0, M)) : L :=
normal(solve(t1 = 0, L)) : eta := ' eta' : f11 := 0 : F[n] := normal(f1) : f1 :=
0 : G[n] := normal(g1) : theta[n] := normal(t1) : g1 := 0 : Feta[n] :=
normal(diff(F[n], eta)) : Geta[n] := normal(diff(G[n], eta)) : theteta[n] :=
normal(diff(theta[n], eta)) : K := ' K' : M := ' M' : L := ' L' : print(F[n]);
print(G[n]); print(theta[n]); od : quit();
```

Some of the stream-function and vorticity are then given as follows:

$$F(\eta) = (2\eta^2 - \eta^4) + \frac{R\eta^2}{36}(\eta^2 - 1)^2(\eta^2 - 10) - \frac{R^2\eta^2}{10800}(\eta^2 - 1)^2(2\eta^6 - 101\eta^4 + 596\eta^2 - 1057) + \frac{R^3\eta^2}{19051200}(\eta^2 - 1)^2(39\eta^{10} - 1287\eta^8 + 33108\eta^6 - 195627\eta^4 + 539468\eta^2 - 731546) + O(R^4) \quad (27)$$

$$G(\eta) = -8\eta + \frac{2R\eta}{3}(2\eta^4 - 12\eta^2 + 7) - \frac{R^2\eta}{135}(3\eta^8 - 105\eta^6 + 408\eta^4 - 705\eta^2 +$$

$$+271) + \frac{R^3 \eta}{113400} (52\eta^{12} - 1365\eta^{10} + 25515\eta^8 - 125300\eta^6 + 275380\eta^4 - 286587\eta^2 + 95360) + O(R^4) \quad (28)$$

The temperature is given by

$$\begin{aligned} \theta(\eta) = & 1 - \frac{PR}{4}(\eta^2 - 1)(\eta^2 - 4) + \frac{PR^2}{288}(\eta^2 - 1)((\eta^2 - 1)^2(\eta^2 - 13) - \\ & - P(32\eta^4 - 175\eta^2 + 257)) - \frac{PR^3}{259200}(\eta^2 - 1)[4(\eta^2 - 1)^2(\eta^6 - 60\eta^4 + \\ & + 417\eta^2 - 918) + P(25\eta^{10} - 794\eta^8 + 9781\eta^6 - 27669\eta^4 + \\ & + 33306\eta^2 - 23169)) + 9P^2(64\eta^8 + 714\eta^6 - 8011\eta^4 + 22714\eta^2 - \\ & - 22261)] + O(R^4) \end{aligned} \quad (29)$$

The wall heat transfer rate, $Nu = -\frac{d\theta}{d\eta}$ at $\eta = 1$ is given by

$$\begin{aligned} Nu = & -\frac{3}{2}PR + P^2R^2 \left(\frac{19}{24} - \frac{71}{1080}R + \frac{163}{8064}R^2 - \frac{9851939}{1306368000}R^3 + \right. \\ & + \frac{199223639}{6466521600}R^4 - \frac{624235571747}{470762772480000}R^5 \left. \right) - P^3R^3 \left(\frac{113}{240} - \frac{3469}{48384}R + \right. \\ & + \frac{9504073}{435456000}R^2 - \frac{1307221193}{172440576000}R^3 + \frac{18264245764741}{6590678814720000}R^4 \left. \right) + \\ & + P^4R^4 \left(\frac{20101}{80640} - \frac{1198187}{20901888}R + \frac{145581581}{8277147648}R^2 - \right. \\ & - \frac{1496749060637}{263627152588800}R^3 \left. \right) - P^5R^5 \left(\frac{3049}{30720} - \frac{3779827813}{114960384000}R + \right. \\ & + \frac{516037495243}{53801459712000}R^2 \left. \right) + P^6R^6 \left(\frac{126437929}{12773376000} - \frac{11175671183}{1434705592320}R \right) + \dots \end{aligned} \quad (30)$$

REFERENCES

1. M. Heil, Stokes Flow in Collapsible Tubes-Computational and Experiment, *Journal of Fluid Mechanics*, 353, 285–312 (1997).
2. O. D. Makinde, Extending the Utility of Perturbation Series in Problems of Laminar Flow in a Porous Pipe and Diverging Channel, *Jour. of Austral. Math. Soc. Ser. B* 41, 118–128 (1999).
3. O. D. Makinde, Heat and Mass Transfer in a Pipe with Moving Surface: Effect of Viscosity Variation and Energy Dissipation, *Quaestiones Mathematicae*. Vol. 24, 97–108 (2001).
4. O. D. Makinde, Collapsible Tube Flow: A Mathematical Model, *Rom. Journ. Phys.*, Vol. 50, Nos. 5–6, 493–506 (2005).
5. O. D. Makinde, Y. A. S. Aregbesola, S. A. Odejide, Wall Driven Steady Flow and Heat Transfer in a Porous Tube, *Kragujevac J. Math.*, 29 193–201 (2006).